



New limits on heavier electroweakinos and their LHC signatures



Amitava Datta^a, Nabanita Ganguly^a, Sujoy Poddar^{b,*}

^a Department of Physics, University of Calcutta, 92 Acharya Prafulla Chandra Road, Kolkata 700009, India

^b Netaji Nagar Day College, 170/436 N.S.C. Bose Road, Kolkata 700092, India

ARTICLE INFO

Article history:

Received 31 August 2016

Received in revised form 15 October 2016

Accepted 15 October 2016

Available online 19 October 2016

Editor: J. Hisano

ABSTRACT

We investigate the heavier electroweakino sectors in several versions of the MSSM, which has not been explored so far in the light of the LHC data, and obtain new bounds using the ATLAS Run I constraints in the $3l + \cancel{E}_T$ channel. We also venture beyond the trilepton events and predict several novel multilepton + \cancel{E}_T signatures of these electroweakinos which may show up during LHC Run II before the next long shutdown. These signals can potentially distinguish between various models with nondecoupled heavier electroweakinos and the much studied ones with decoupled heavier electroweakinos.

© 2016 The Authors. Published by Elsevier B.V. This is an open access article under the CC BY license (<http://creativecommons.org/licenses/by/4.0/>). Funded by SCOAP³.

The null results from the searches for supersymmetry (SUSY) [1] during Run I of the LHC have imposed stringent bounds on the masses of the strongly interacting supersymmetric particles (sparticles) [2,3], some of which have been further strengthened by the preliminary results from the Run II at 13 TeV. This trend naturally provokes a close scrutiny of a scenario where all the strongly interacting sparticles are beyond the reach of the experiments before the next shutdown. If this indeed be the case then the prospective SUSY signals during the next few years will be governed by the electroweak (EW) sector. It is also worth recalling that this sector alone accounts for several phenomenological triumphs of SUSY like explanation of the observed dark matter (DM) relic density of the universe [4–6], alleviation of the tension between the precisely measured value of the anomalous magnetic moment of the muon [7] and the SM prediction [8].

In the R-parity conserving Minimal Supersymmetric Standard Model (MSSM) without any assumption regarding the soft SUSY breaking mechanism, the fermionic sparticles in the EW sector are the charginos ($\tilde{\chi}_j^\pm$, $j = 1 - 2$) and the neutralinos ($\tilde{\chi}_i^0$, $i = 1 - 4$)—collectively called the electroweakinos (eweakinos). In the MSSM the masses and the compositions of these sparticles are determined by four independent parameters: the U(1) gaugino mass parameter M_1 , the SU(2) gaugino mass parameter M_2 , the higgsino mass parameter μ and $\tan \beta$, the ratio of the vacuum expectation values of the two neutral Higgs bosons. Throughout this paper we take $\tan \beta = 30$ which usually gives a better agreement with the $(g - 2)_\mu$ data. The indices j and i are arranged in ascending or-

der of the masses. The stable, neutral lightest neutralino ($\tilde{\chi}_1^0$) is a popular DM candidate. The scalar sparticles are the L and R type sleptons and the sneutrinos. We assume L (R)-type sleptons of all flavours to be mass degenerate with a common mass $m_{\tilde{L}}$ ($m_{\tilde{R}}$). Because of SU(2) symmetry the sneutrinos are mass degenerate with L -sleptons modulo the D-term contribution. We neglect LR mixing in the slepton sector. For simplicity we work in the decoupling regime of the Higgs sector of the MSSM with only one light, SM like Higgs boson [9], a scenario consistent with all Higgs data collected so far [10].

During Run I the eweakino searches were mainly based on the hadronically quiet $3l + \cancel{E}_T$ signal.¹ The null results from these searches were interpreted by the LHC collaborations in terms of several simplified models consisting of a minimal set of parameters required to study this signal. It was, e.g., assumed in all analyses that the $3l$ signal comes only from $\tilde{\chi}_1^\pm - \tilde{\chi}_2^0$ production followed by their leptonic decays [11,12] while the heavier eweakinos are decoupled. This resulted in correlated bounds on $m_{\tilde{\chi}_1^\pm}$ and $m_{\tilde{\chi}_1^0}$. In contrast in [13–15] the data was reinterpreted in terms of different MSSMs some of which are closely related to the above simplified models. In each case the full set of parameters belonging to the EW sector are specified so that one can also address other important issues like the DM relic density, the correlation among the trilepton and slepton search data etc.

In this letter we emphasize the potential signatures of the hitherto unexplored heavier eweakinos in the upcoming LHC experiments at 13 TeV before the next shutdown. That these signals are indeed well within the reach of the ongoing experiments is

* Corresponding author.

E-mail addresses: adatta_ju@yahoo.co.in (A. Datta), nabanita.rimpi@gmail.com (N. Ganguly), sujoy.phy@gmail.com (S. Poddar).

¹ In this paper l stands for e and μ unless otherwise mentioned.

indicated by the observation that the published bounds on the lighter eweakinos masses from Run I turn out to be quite sensitive to the masses of heavier eweakinos. This we shall show below by relaxing the ad hoc assumption of strict decoupling. The rich phenomenology of the non-decoupled scenarios is further illustrated by some novel signatures like events with 4l s, three same sign and one opposite sign (SS3OS1) leptons and 5l s, all accompanied by large \cancel{E}_T , which may be observed with $\lesssim 100 \text{ fb}^{-1}$ of luminosity i.e., before the next long shutdown. Most important: for a compressed lighter eweakino spectrum all viable leptonic signals including the 3l events are due to the heavier ones. In addition in a wide variety of non-compressed models the source of m-lepton signals with $m > 3$ are the non-decoupled heavier eweakinos.

The constraints from the trilepton searches are also sensitive to the composition of the eweakinos. The analyses are mainly restricted to two generic scenarios.²

a) The Light Wino (LW) models: Many analyses assume that the $\tilde{\chi}_1^\pm$ and $\tilde{\chi}_2^0$ are purely wino and nearly mass degenerate while the $\tilde{\chi}_1^0$ is bino dominated [11–13]. These two lighter eweakinos have closely spaced masses governed by the parameter M_2 while the $\tilde{\chi}_1^0$ is either bino dominated with mass controlled by the U(1) gaugino mass parameter M_1 or a bino-higgsino admixture ($M_1 \lesssim \mu$). The two heavier electroweakinos are higgsino like with masses approximately equal to μ , where $M_2 < \mu$

b) The Light Higgsino (LH) models: In contrast this paper, following Ref. [14], mainly addresses scenarios with higgsino dominated $\tilde{\chi}_1^\pm$, $\tilde{\chi}_2^0$ and $\tilde{\chi}_3^0$ while the LSP is either bino dominated or a bino-higgsino admixture. The three lighter eweakinos have closely spaced masses governed by μ while the $\tilde{\chi}_1^0$ is either bino dominated with mass controlled by M_1 or a bino-higgsino admixture ($M_1 \lesssim \mu$). The two heavier electroweakinos are wino like with masses approximately equal to M_2 , where $M_2 > \mu$.

We recall that the models belonging to class a) (b)) yield stronger (weaker) mass bounds for reasons explained in [14]. In all models the trilepton rates also depend sensitively on the hierarchy among the slepton and eweakino masses. If the sleptons are lighter (heavier) than $\tilde{\chi}_1^\pm$ and $\tilde{\chi}_2^0$, the leptonic Branching Ratios (BR) of these eweakinos are typically large (small) yielding stronger (weaker) limits. The nomenclatures introduced in [14] also indicate this hierarchy (e.g., Light Wino and light Left Slepton (LWLS) model, Light Higgsino and Heavy Slepton (LHHS) model etc.). In the LHHS model both L and R type sleptons of all flavours are heavier than $\tilde{\chi}_1^\pm$ and $\tilde{\chi}_2^0$.

We now derive the new limits in different models following the procedure of the ATLAS collaboration [11]. The Tables 7 and 8 of [11] contain the number of observed 3l + \cancel{E}_T events and the SM backgrounds obtained from the data for a number of signal regions (see Table 4 in [11]). Each signal region is characterized by a set of kinematical cuts. From these information the model independent 95% CL upper limit on any Beyond SM (BSM) events (N_{obs}^{95}) for each signal region were computed and displayed in the same tables. Using these upper bounds the ATLAS group obtained an exclusion contour in a simplified LWLS model (see Fig. 7a of [11]). We validate our simulation by reproducing this exclusion contour and proceed to obtain new constraints in several models with non-decoupled heavier eweakinos.³

We generate the SUSY spectrum using SUSYHIT [16] and simulate the signal events using PYTHIA (v6.4) [17] (for the details see [13,14]). We use CTEQ6L [18] for parton distribution functions in all our analyses. Jets are reconstructed by the anti- k_r [19] al-

gorithm using FASTJET [20] coupled with PYTHIA with $R = 0.4$. The jets are required to have $P_T \geq 20 \text{ GeV}$ and $|\eta| < 2.5$. In all our analyses the following lepton selection criteria have been employed: i) All leptons (e and μ) in the final state with pseudorapidity $|\eta| < 2.5$ and transverse momentum $P_T > 10 \text{ GeV}$ are selected. ii) Each lepton is required to pass the isolation cuts as defined by the ATLAS/CMS collaborations [11,12]. These selection cuts have been implemented in all analyses in this paper.

We obtain the most striking consequences in the LHHS model yielding the weakest bounds on the higgsino like lighter eweakinos— $\tilde{\chi}_1^\pm$, $\tilde{\chi}_2^0$ and $\tilde{\chi}_3^0$ [14]. Naturally the possibility that the heavier eweakinos ($\tilde{\chi}_2^\pm$ and $\tilde{\chi}_4^0$) also have relatively small masses is open in this case. They are wino like with masses approximately equal to the SU(2) gaugino mass parameter M_2 , where $M_2 > \mu$. For this class of models the common slepton mass is chosen to be $m_{\tilde{L}} = m_{\tilde{R}} = (m_{\tilde{\chi}_1^\pm} + m_{\tilde{\chi}_2^\pm})/2$ so that they are always lighter (heavier) than the heavier (lighter) eweakinos. The slepton and the LSP masses are carefully chosen in all our analyses that they are consistent with the constraints from Run I direct slepton searches [21].

If the lighter eweakino spectrum is compressed, i.e., $M_1 \approx \mu$, then $\tilde{\chi}_1^\pm$, $\tilde{\chi}_1^0$, $\tilde{\chi}_2^0$ and $\tilde{\chi}_3^0$ have large bino and higgsino components and are approximately degenerate. For all numerical computations we take $\mu = 1.05 M_1$. Consequently the 3l + \cancel{E}_T or any other leptonic signal from $\tilde{\chi}_1^\pm - \tilde{\chi}_2^0$ (or $\tilde{\chi}_3^0$) production is not viable since the energy release in each underlying decay is small. On the other hand it is known for a long time that an LSP which is a bino-higgsino admixture is attractive both from the point of view of the observed DM relic density of the universe and naturalness ([22,23]). The correlation between acceptable DM relic density and the 3l signal in the compressed scenario with decoupled $\tilde{\chi}_2^\pm$ and $\tilde{\chi}_4^0$ ($M_2 \simeq 2\mu$) can be understood from the LHHS model discussed in [14]. From Fig. 5 of [14], it follows that annihilation and co-annihilation of a bino-higgsino LSP produce acceptable DM relic density over a parameter space where the 3l signal is weak. We have checked that if the above sparticles are non-decoupled ($M_2 < 2\mu$) the parameter space allowed by the WMAP and Planck data changes very little. Acceptable relic density, e.g., is obtained for the range $1.05\mu \leq M_2 \leq 1.5\mu$ a part of which also yields novel LHC signals.⁴

The above tension eases out if the heavier eweakinos are not decoupled. In this case the wino like $\tilde{\chi}_2^\pm$ and $\tilde{\chi}_4^0$ are pair produced with reasonably large cross-sections over a sizable portion of the parameter space. Moreover their 2-body leptonic decays via sleptons with large BRs are potential sources of observable trilepton signals. Using the above ATLAS upper bounds on N_{obs}^{95} , we obtain the first published exclusion contour in the $m_{\tilde{\chi}_1^0} - m_{\tilde{\chi}_2^\pm}$ plane (Fig. 1). For $m_{\tilde{\chi}_1^0} \approx 80 \text{ GeV}$ below which $m_{\tilde{\chi}_1^\pm}$ violates the LEP bound, there is a strong bound $m_{\tilde{\chi}_2^\pm} > 610 \text{ GeV}$. On the other hand for $m_{\tilde{\chi}_1^0} \geq 170 \text{ GeV}$, there is no bound on $m_{\tilde{\chi}_2^\pm}$. For $m_{\tilde{\chi}_2^\pm} \lesssim 300 \text{ GeV}$, $\tilde{\chi}_2^\pm$ and $\tilde{\chi}_4^0$ develop significant bino-higgsino component and the constraints weaken. Below $m_{\tilde{\chi}_2^\pm} \approx 250 \text{ GeV}$ all the eweakinos are approximately degenerate and the model cannot be constrained any further. For illustrating the signatures of this compressed model at LHC Run II we have chosen the benchmark point BP1 which is presented in Table 1 along with the corresponding bound on $m_{\tilde{\chi}_2^\pm}$.

⁴ We note in passing that the proposed LHC signatures of compressed scenarios with decoupled heavier eweakinos have so far been based on the monojet + \cancel{E}_T topology or the vector boson fusion topology with forward jet tagging ([24–28]). However, revealing the underlying physics with these signatures alone will indeed be impossible.

² We shall, however, briefly comment on other models as well.

³ An earlier example of the reliability of our simulation is presented in Fig. 7a of [13]. See also [15], Fig. 6.

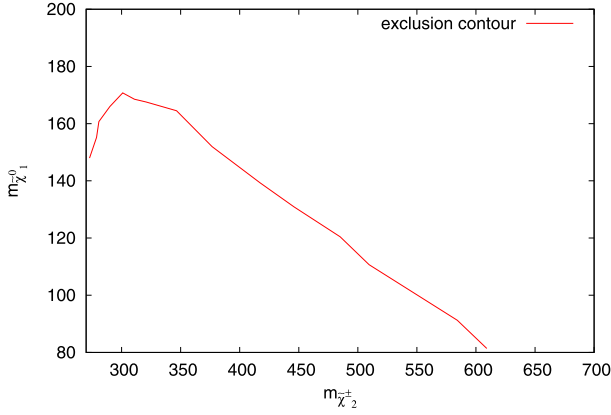


Fig. 1. The red contour represents the excluded parameter space in the $m_{\tilde{\chi}_2^\pm} - m_{\tilde{\chi}_1^0}$ plane using ATLAS trilepton search data from LHC RUN I. Instead of following the usual practise of considering $\tilde{\chi}_1^\pm - \tilde{\chi}_2^0$ production only we have taken into account all possible eweakino pair production in the compressed LHHS model (see text for the details). All masses are in GeV. (For interpretation of the references to colour in this figure, the reader is referred to the web version of this article.)

In order to get a preliminary estimate of the reach of Run II experiments at 13 TeV via the $3l + \cancel{E}_T$ channel we have simulated the signal and all SM processes considered as backgrounds in the ATLAS $3l$ analysis reported above. The backgrounds are suppressed by selecting events with

- A1) 3 isolated leptons consistent with the selection cuts mentioned above,
- A2) invariant mass of any pair of oppositely charged leptons of same flavour not in the window $81.2 < m_{inv} < 101.2$ GeV, and
- A3) $\cancel{E}_T > 200$ GeV.

The total SM background is estimated to be 26.71 for an integrated luminosity of 100 fb^{-1} . Taking $S/\sqrt{B} \geq 5$ to be an indicator of the observability of the signal, we find that for $m_{\tilde{\chi}_1^0} = 80$ (250) GeV, the reach in the compressed model is $m_{\tilde{\chi}_2^\pm} = 820$ (672) GeV for 100 fb^{-1} of integrated luminosity. Thus much higher $m_{\tilde{\chi}_2^\pm}$ can indeed be probed even for $m_{\tilde{\chi}_1^0}$ beyond the reach of Run I. Moreover it is natural to expect that when the background is more accurately measured from the data the actual mass reach can be improved by optimizing the cuts.

In the absence of the above compression both lighter and heavier eweakinos can in principle contribute to the $3l$ signal. This is illustrated by the constraints derived for BP2 and BP3 (Table 1). It follows from these examples that for a fixed M_2 ($m_{\tilde{\chi}_1^\pm}$) one can constrain the free parameter $m_{\tilde{\chi}_1^\pm}$ ($m_{\tilde{\chi}_2^\pm}$) as is illustrated by BP2 (BP3). It is worth recalling that for decoupled heavier eweakinos there was no limit on the lighter eweakinos for $m_{\tilde{\chi}_1^0} \approx 100$ GeV as is the case in both the examples (see [14], Fig. 5).⁵ The main message of this analysis is that a large portion of the parameter space with non-decoupled $\tilde{\chi}_2^\pm$, $\tilde{\chi}_4^0$ had in principle been within the kinematical reach of the Run I experiments. It is, therefore, natural to seriously consider the possibility that they may show up even in the early phases of the experiments at 13 TeV. Especially if a signal shows up, both the lighter and heavier eweakinos would demand serious attention in the race for revealing the underlying physics.

Stronger new bounds are also obtained in the Light Higgsino and light Left Slepton (LHLS) model (Fig. 3b of [14]). In this sce-

Table 1

New (modified) limits on $m_{\tilde{\chi}_2^\pm}(m_{\tilde{\chi}_1^\pm})$ for fixed $\tilde{\chi}_1^\pm(M_2)$ in different models with non-decoupled $\tilde{\chi}_2^\pm$ and $\tilde{\chi}_4^0$. All masses and mass parameters are in GeV. ‘-’ denotes that the corresponding mass parameters are treated as free parameters and ‘*’ indicates that the corresponding $m_{\tilde{\chi}_2^\pm}$ is determined by M_2 and the lower limit on $m_{\tilde{\chi}_1^\pm}$. The modified limits on $m_{\tilde{\chi}_1^\pm}$ are stronger than the corresponding limits in the decoupled scenario.

Parameters/ Masses	BP1 (LHHS)	BP2 (LHHS)	BP3 (LHHS)	BP4 (LHLS)	BP5 (LMLS)
M_1	191	105	105	175	296
μ	$\simeq M_1$	-	264	-	$1.05M_2$
M_2	-	1.5μ	-	1.5μ	566
$m_{\tilde{\chi}_1^0}$	152	100	100	170	290
$m_{\tilde{\chi}_1^\pm}$	178	> 250	250	> 400	> 540
$m_{\tilde{\chi}_2^\pm}$	> 370	*	> 415	*	*

nario only the left sleptons are assumed to be lighter than $\tilde{\chi}_1^\pm$ and $\tilde{\chi}_2^0$. Following [11] and [14] their masses are chosen to be $m_{\tilde{L}_i} = (m_{\tilde{\chi}_1^\pm} + m_{\tilde{\chi}_1^0})/2$. The limit $m_{\tilde{\chi}_1^\pm} > 400.0$ GeV corresponds to BP4 (Table 1) with $M_2 = 1.5\mu$ and $m_{\tilde{\chi}_1^0} = 170$ GeV. For this $m_{\tilde{\chi}_1^0}$ and decoupled heavier eweakinos (i.e., M_2 having a significantly larger value) a much weaker bound $m_{\tilde{\chi}_1^\pm} > 270.0$ GeV was obtained ([14], Fig. 3b).

In the Light Mixed and light Left Slepton (LMLS) model we have $M_2 \approx \mu$ and the LSP is a bino ($M_1 < \mu$) (Fig. 4b in [14]). The left slepton masses are chosen as in the LHLS model. It follows from these examples that for a fixed M_2 one can constrain the free parameter $m_{\tilde{\chi}_1^\pm}$ (see BP5). For the chosen LSP mass there is no limit on $m_{\tilde{\chi}_1^\pm}$ for decoupled heavier eweakinos.

The above results encourage us to look into the multilepton + \cancel{E}_T signatures in models with non-decoupled heavier eweakinos at LHC 13 TeV experiments. We begin with the $4l + \cancel{E}_T$ signal. It may be recalled that the ATLAS collaboration analysed this signal towards the end of Run I assuming decoupled heavier eweakinos [29] for a RPC simplified model assuming that the signal comes only from higgsino like $\tilde{\chi}_2^0 - \tilde{\chi}_3^0$ pair production. It was further assumed that they decay via any one of the following options: i) R -type selectrons or smuons, ii) staus or iii) Z bosons with 100% BR. In contrast our broader framework considers all eweakino pair productions in several generic MSSM models each represented by a BP displayed in Table 2. These BPs correspond to diverse compositions of the eweakinos, different mass hierarchies among the EW sparticles and realistic BRs of the relevant decay modes. All BPs are consistent with the new constraints derived in this paper for non-decoupled $\tilde{\chi}_2^\pm$ and $\tilde{\chi}_4^0$ (Fig. 1 and Table 1).

An obvious physics background in this case is ZZ production. We have generated ZZ + 1 jet events with MLM matching [30] using ALPGEN(v2.1) [31] which are then passed to PYTHIA for showering and jet formation using the anti- k_t algorithm [19]. We have simulated the signal and all SM backgrounds by selecting events with

- B1) 4 isolated leptons consistent with the selection cuts mentioned above,
- B2) Invariant mass of any pair of oppositely charged leptons of same flavour not in the window $81.2 < m_{inv} < 101.2$ GeV, and
- B3) $\cancel{E}_T > 80.0$ GeV.

In Table 2 we have presented the relevant parameters defining each BP in rows 2–7. The number of $4l$ events $N(4l)$ for 100 fb^{-1} of integrated luminosity subject to the above cuts for each BP and the total SM background are in row 9. For a better under-

⁵ We confirm the validity of this result with the latest constraints [11] which are somewhat stronger than the earlier ones used in [14].

Table 2

Number of $3l$, $4l$, $SS3OS1$, $5l$ events all with \cancel{E}_T corresponding to different BPs at LHC 13 TeV for integrated luminosity of 100 fb^{-1} along with the total SM background in each case. The significance of the $3l$ signal is also shown for each BP. The contents of the brackets are numbers in the corresponding decoupled scenario which are significantly smaller. All masses and mass parameters are in GeV.

Parameters/Masses and Signals	BP1 (LHHS)	BP2 (LHHS)	BP3 (LHHS)	BP4 (LHHS)	BP5 (LHHS)	BP6 (LHLS)	BP7 (LMLS)	Total SM Backgrounds
M_1	191	222	132	105	104	249	321	–
μ	186	268	133	270	308	300	401	–
M_2	350	286	486	405	462	450	382	–
$m_{\tilde{\chi}_1^0}$	151	200	100	100	100	231	305	–
$m_{\tilde{\chi}_1^\pm}$	178	234	132	260	300	291	350	–
$m_{\tilde{\chi}_2^\pm}$	389 (885)	351 (880)	520 (890)	447 (810)	504 (927)	491 (902)	465	–
3 leptons	73.8 (17.3)	35.9 (12.0)	107.7 (17.1)	70.4 (16.1)	56.4 (7.84)	139.4 (21.9)	58.2 (30.9)	26.71
$(S/\sqrt{B})_{3l}$	14.3 (3.35)	6.95 (2.32)	20.8 (3.31)	13.6 (3.12)	10.9 (1.52)	26.9 (4.24)	11.3 (5.98)	–
4 leptons	61.5 (0.69)	52.5 (1.20)	51.7 (–)	16.4 (0.62)	8.73 (0.36)	19.6 (2.05)	10.2 (–)	0.835
SS3OS1 leptons	29.9 (0.69)	17.1 (0.30)	14.5 (–)	7.2 (–)	3.36 (0.36)	5.01 (0.17)	1.57 (–)	0.40
5 leptons	8.46 (–)	8.29 (0.60)	4.14 (–)	6.1 (–)	2.68 (–)	4.14 (–)	0.78 (–)	0.60

Table 3

The production cross sections of all eweakino pairs and the effective cross-section after successive cuts of four types of signals for the BPs defined in Table 2. The contents of the brackets are numbers in the corresponding decoupled scenarios.

Benchmark Points	σ_{prod} in pb	σ_{eff}^{3l} in fb			σ_{eff}^{4l} in fb			σ_{eff}^{SS3OS1} in fb		σ_{eff}^{5l} in fb	
		after A1	after A2	after A3	after B1	after B2	after B3	after C1	after C2	after D1	after D2
BP1	769.1 (691.6)	8.96	7.54	0.74	1.42	1.01	0.62	0.38	0.30	0.15	0.08
BP2	553.0 (300.7)	10.5	8.09	0.36	1.68	1.06	0.51	0.39	0.17	0.19	0.07
BP3	2071.0 (2060.0)	7.08	6.65	1.08	0.74	0.62	0.52	0.16	0.14	0.06	0.04
BP4	380.8 (309.1)	5.06	2.87	0.70	0.45	0.22	0.16	0.09	0.07	0.08	0.06
BP5	223.7 (182.3)	2.86	1.67	0.56	0.28	0.11	0.09	0.04	0.03	0.03	0.026
BP6	217.9 (170.9)	15.9	14.6	1.39	0.51	0.40	0.20	0.06	0.05	0.05	0.04
BP7	156.9 (72.6)	12.3	11.1	0.58	0.30	0.19	0.10	0.02	0.015	0.03	0.0078

standing of these numbers the total production cross section of all chargino neutralino pairs in each case and the corresponding effective cross sections (σ_{eff}^{4l}) after the cuts B1)–B3) are given in columns 2 and 6–8 Table 3. The total background cross section and the effective cross sections after the cuts for different channels are in Table 4. The total background is indeed tiny. If we require at least five signal events over a negligible background for a discovery, then optimistic results are obtained for all BPs. On the other hand the number in parenthesis below each $N(4l)$ stands for the corresponding number in the decoupled scenario. The numerical results in the non-decoupled (decoupled) models are obtained for $M_2 = 1.5\mu$ ($M_2 = 2\mu$). It is clear that in a variety of decoupled models the $N(4l)$ is indeed negligible.

Two comments are now in order. For the $t(\bar{t})Z$ a NLO corrected cross-section boosted by a K-factor of 1.35 [32] yields about 5 background events. In order suppress it further we have used an additional cut. We reject events with at least one tagged b -jet following the criteria MV1 of [33] and the effective cross-section in

Table 4 is reduced to 0.004 fb. The signal is hardly affected by this additional cut. The irreducible backgrounds being negligible one has to look for the reducible backgrounds arising due to jets faking leptons. Without a thorough detector simulation it is difficult to estimate this background. The analysis of [29], however, found this background to be negligible for the $4l + \cancel{E}_T$ signal. It is, therefore, reasonable to assume that this background is negligible for all the signals with four or more leptons considered in this paper.

For comparison we also present in Table 2 the number of $3l + \cancel{E}_T$ events $N(3l)$ obtained with the cuts A1)–A3) defined above and the total SM background for an integrated luminosity of 100 fb^{-1} (row 8). The production cross section of all chargino-neutralino pairs, the effective cross sections after the cuts for both the signal the total background etc are also included in Tables 3–4 following the same convention as in the $4l$ case. It readily follows from Table 2 the ratio N_{4l}/N_{3l} , which is free from several theoretical uncertainties, one can discriminate between many non-decoupled and decoupled models since the ratio is tiny in a wide

Table 4

The production and effective cross-sections of different SM backgrounds for the four different signals. ‘-’ denotes that the concerned background process is not relevant for the signal.

Background Processes	σ_{prod} in pb	σ_{eff}^{3l} in fb			σ_{eff}^{4l} in fb			σ_{eff}^{SS3OS1} in fb		σ_{eff}^{5l} in fb	
		after A1	after A2	after A3	after B1	after B2	after B3	after C1	after C2	after D1	after D2
WZ	32.69	168.3	13.11	0.18	-	-	-	-	-	-	-
ZZ	10.63	16.5	1.25	0.007	14.2	0.081	0	-	-	-	-
$t\bar{t}Z$	0.018	1.95	0.39	0.015	0.26	0.039	0.018	0.006	0.002	0.002	0.0007
WWZ	0.133	1.33	0.17	0.013	0.18	0.012	0.004	-	-	-	-
WZZ	0.042	0.54	0.044	0.005	0.068	0.0014	0.0003	0.007	0.003	0.013	0.005
ZZZ	0.010	0.05	0.003	0.0001	0.04	0.0003	0.00005	0.0004	0.00003	0.001	0.0003
WWW	0.159	0.79	0.07	0.059	-	-	-	-	-	-	-

variety of decoupled models. The same observable may also be useful for discriminating among the non-decoupled models. Similar relative rates involving other final states (see below) can also be used to facilitate this discrimination.

The same methodology has been followed for generating the $SS3OS1 + \cancel{E}_T$ signal which is a subset of the $4l + \cancel{E}_T$ events. However, this choice of the final state significantly reduces the backgrounds involving multiple Z bosons or $t\bar{t}Z$. The main irreducible SM background in this case are WZZ events where a lepton from any Z boson decay fails to pass the selection cuts. The selection cuts (C_1) and the cut $\cancel{E}_T > 80$ GeV (C_2) suppress this and other backgrounds listed in Table 4 to negligible levels. The number of signal events for an integrated luminosity of 100 fb^{-1} corresponding to the above BPs are displayed in Table 2. The relevant information about the effective signal cross sections can be gleaned from the Table 3. It may be noted that the relative rates of $4l$ and $SS3OS1$ events can distinguish among different decoupled models.

The next entry in our list is the $5l + \cancel{E}_T$ signal, where l stands for an e or μ of any charge. The selection cuts (D1) and the requirement $\cancel{E}_T > 80$ GeV (D2) cut suppress all the backgrounds including the potentially dangerous contribution from WZZ events to a negligible level. We quote the number of signal events for the BPs studied and the total background for an integrated luminosity of 100 fb^{-1} in Table 2.

We now briefly comment on the signals in the LWLS model which yielded the strongest bounds on the lighter eweakinos (see Fig. 7a of [11]). For $m_{\tilde{\chi}_1^0} \leq 250$ GeV one obtains $m_{\tilde{\chi}_1^\pm} \geq 700$ GeV. In this case the heavier eweakinos are too massive to produce any observable signal before the LHC luminosity upgrade. However, if the lighter eweakino spectrum is to some extent compressed the above stringent bound on $m_{\tilde{\chi}_1^\pm}$ is relaxed. This is illustrated by the following parameter set: $M_1 = 298.0$, $M_2 = 345.0$, $\mu = 518.0$, $m_{\tilde{\chi}_1^0} = 290.0$, $m_{\tilde{\chi}_1^\pm} = 349.0$ and $m_{\tilde{\chi}_2^\pm} = 545.0$ (all in GeV). In this scenario the number of $4l$ events and $SS3OS1$ events are respectively 9.37 and 3.33 for 100 fb^{-1} of integrated luminosity with the above cuts.

The potentially rich phenomenology of the heavier eweakinos calls for further investigations in the light of the upcoming LHC data, the observed DM relic density of the universe and the $(g-2)_\mu$ anomaly. We have already checked that they may significantly contribute to $(g-2)_\mu$. Further details will be provided elsewhere.

Acknowledgements

The research of AD was supported by the Indian National Science Academy, New Delhi. NG thanks the Board of Research in

Nuclear Sciences, Department of Atomic Energy, India for a research fellowship.

References

- [1] For reviews on supersymmetry, see, e.g., H.P. Nilles, Phys. Rep. 110 (1984) 1; H.E. Haber, G. Kane, Phys. Rep. 117 (1985) 75; D.J.H. Chung, et al., Phys. Rep. 407 (2005) 1; S.P. Martin, arXiv:hep-ph/9709356.
- [2] See the web, <https://twiki.cern.ch/twiki/bin/view/AtlasPublic/SupersymmetryPublicResults>.
- [3] See the web, <https://twiki.cern.ch/twiki/bin/view/CMSPublic/PhysicsResultsSUS>.
- [4] G. Hinshaw, et al., arXiv:1212.5226 [WMAP Collaboration].
- [5] P.A.R. Ade, et al., Planck Collaboration, Astron. Astrophys. 571 (2014) A16.
- [6] For reviews on darkmatter, see, e.g., C. Jungman, M. Kamionkowski, K. Griest, Phys. Rep. 267 (1996) 195; G. Bertone, D. Hooper, J. Silk, Phys. Rep. 405 (2005) 279.
- [7] G.W. Bwnnett, et al., Muon G-2 Collaboration, Phys. Rev. D 73 (2006) 072003; B.L. Roberts, Chin. Phys. C 34 (2010) 741.
- [8] K. Hagiwara, R. Liao, A.D. Martin, D. Nomura, T. Teubner, J. Phys. G 38 (2011) 085003; F. Jegerlehner, A. Nyffeler, Phys. Rep. 477 (2009) 1.
- [9] See, e.g., A. Djouadi, Phys. Rep. 459 (2008) 1.
- [10] See, e.g., Philip Bechtle, et al., arXiv:1608.00638 [hep-ph].
- [11] G. Aad, et al., ATLAS Collaboration, J. High Energy Phys. 1404 (2014) 169.
- [12] V. Khachatryan, et al., CMS Collaboration, Phys. Rev. D 90 (2014) 092007.
- [13] M. Chakraborti, U. Chattopadhyay, A. Choudhury, A. Datta, S. Poddar, J. High Energy Phys. 1407 (2014) 019.
- [14] M. Chakraborti, U. Chattopadhyay, A. Choudhury, A. Datta, S. Poddar, J. High Energy Phys. 1511 (2015) 050.
- [15] A. Choudhury, S. Mondal, Phys. Rev. D 94 (5) (2016) 055024.
- [16] A. Djouadi, M.M. Muhlleitner, M. Spira, Acta Phys. Pol. B 38 (2007) 635.
- [17] T. Sjostrand, S. Mrenna, P. Skands, J. High Energy Phys. 05 (2006) 026.
- [18] J. Pumplin, D. Stump, J. Huston, H. Lai, P.M. Nadolsky, et al., J. High Energy Phys. 0207 (2002) 012.
- [19] M. Cacciari, G.P. Salam, G. Soyez, J. High Energy Phys. 0804 (2008) 063.
- [20] M. Cacciari, G.P. Salam, G. Soyez, Eur. Phys. J. C 72 (2012) 1896.
- [21] G. Aad, et al., ATLAS Collaboration, J. High Energy Phys. 1405 (2014) 071.
- [22] N. Arkani-Hamed, A. Delgado, G.F. Giudice, Nucl. Phys. B 741 (2006) 108–130.
- [23] H. Baer, A. Mustafayev, E. Park, X. Tata, J. Cosmol. Astropart. Phys. 0701 (2007) 017.
- [24] G.F. Giudice, T. Han, K. Wang, L. Wang, Phys. Rev. D 81 (2010) 115011.
- [25] P. Schwaller, J. Zurita, J. High Energy Phys. 1403 (2014) 060.
- [26] Z. Han, G.D. Kribs, A. Martin, A. Menon, Phys. Rev. D 89 (7) (2014) 075007.
- [27] H. Baer, A. Mustafayev, X. Tata, Phys. Rev. D 90 (11) (2014) 115007.
- [28] V. Khachatryan, et al., CMS Collaboration, Phys. Lett. B 759 (2016) 9–35.
- [29] G. Aad, et al., ATLAS Collaboration, Phys. Rev. D 90 (2014) 052001.
- [30] M. Mangano, M. Moretti, F. Piccinini, M. Treccan, J. High Energy Phys. 0701 (2007) 013; S. Hoeche, F. Krauss, N. Lavesson, L. Lonnblad, M. Mangano, arXiv:hep-ph/0602031.
- [31] M. Mangano, et al., J. High Energy Phys. 0307 (2003) 001.
- [32] A. Lazopoulos, T. McElmurry, K. Melnikov, F. Petriello, Phys. Lett. B 666 (2008) 62.
- [33] G. Aad, et al., ATLAS Collaboration, ATLAS-CONF-2012-043.